

**Modeling and Optimization of an Industrial
Glass Furnace**

M. G. Carvalho, P. Oliviera, and V. Semião

Reprinted from **Dynamics of Reactive Systems Part II: Heterogeneous Combustion and Applications**, edited by A. L. Kuhl, J. R. Bowen, J.-C. Leyer, and A. Borisov, Vol. 113 of *Progress in Astronautics and Aeronautics*, AIAA, Washington, DC, ISBN 0-930403-46-0, 1988.

Nomenclature

g_i	= gravitational acceleration in the i -direction
K_{eff}	= effective thermal conductivity of the glass
p	= pressure
S_T	= source term of temperature equation
T	= temperature
u_i	= velocity component in the i -direction
x_j	= co-ordinate direction
Γ_T	= molecular exchange coefficient for temperature
δ_{ij}	= Kronecker's delta
μ	= molecular viscosity
ρ	= time-mean density

I. Introduction

A. Preamble

The recent awareness of the limitation of energy resources, the increase in fuel prices, and the problem of pollution have turned the combustion engineers' attention toward the importance of improving the combustion equipment design.

There is currently considerable interest from the glass and ceramic industry to support the construction of a mathematical model that reliably simulates the performance of the glass melting furnaces. Glass furnaces are large and are thus extremely costly to develop by highly empirical methods.

Most of the previous glass furnace predictive studies have avoided the complexities of the combustion chamber region and have confined their attention to the flow in the tank [see Chen and Goodson (1972), Suzuki (1976), and Oliveira (1986), for example].

A three-dimensional simulation of a glass furnace combustion chamber in which the flowfield and heat release were determined from a numerical solution of the governing balance equations was presented by Gosman et al. (1980). The works of Carvalho (1983) and Semião (1986) have extended the work of Gosman et al. (1980) to more complex geometries with a horseshoe flow shape. The predictions of Semião (1986) were made to oxygen-rich burning conditions. The work of

Carvalho et al. (1987) is an extension of Semião (1986) in which the authors have used a two-dimensional axisymmetric model to simulate the burner region providing with these results the inlet conditions for the three-dimensional calculations of the combustion chamber. The results were extensively validated with experimental data acquired in the referred furnace (Carvalho et al. 1988-a).

There have been very few attempts to model a complete glass furnace. A simplified model was presented by McConnell and Goodson (1979) in which global energy equations for the combustion chamber, molten glass, and feed ("batch") were solved for an assumed flow and heat release, with Hottel's zone method employed to calculate the combustion chamber radiation. A similar study was effected by Mase and Oda (1980), but the flowfield in the molten glass was solved assuming two-dimensionality. A further study of this kind has been performed by a study by Novak (1980), in which the combustion chamber flowfield was more carefully estimated with the assistance of empirical data for nonreacting flows for cylindrical ducts. The study of Carvalho and Lockwood (1985) extended the work presented in Carvalho (1983) to an industrial furnace of differing configuration and brought into analysis the batch and glass tank flows assuming two-dimensionality of the batch flow. The glass tank flow predictions were made with a three-dimensional computer procedure.

The present work deals with a completely three-dimensional simulation of an industrial glass furnace, extending the work of Carvalho et al. (1988-b) to the improvement of an industrial glass furnace design. Predictions were made for a wide range of parameters of the combustion chamber, and their effects on the furnace are quantified in a demonstration of the abilities of the procedure. The main feature of the combustion chamber of the predicted furnace, under real operating conditions, was the poor mixing pattern between oxygen and fuel as a consequence of the inlet port design, namely the position of the fuel injector [see Carvalho et al. (1988-b)]. For this reason, there was a small amount of wasted unburned fuel at the outlet. To enhance the combustion chamber performance, several runs were made and the results are presented in this paper. The excess air and preheat levels were varied, and a better position of the fuel injection was sought.

The combustion chamber and the molten glass flow were studied by a cyclical iterative way, by separated calculations, matched by the relation between the heat flux from the flame to the glass surface and its temperature. Assuming known values of the temperature of the glass surface, the flow, combustion process, and heat fluxes were predicted by

a three-dimensional solution technique, which forms the first submodel. Using the calculated heat flux toward the glass as a boundary condition, the flow and the temperature distribution of the molten glass were predicted by a different three-dimensional numerical technique, which forms the second submodel. These glass surface temperatures were then introduced as a boundary condition in the first submodel, framing a cyclical iterative procedure that "converged" solution allows one to predict the performance of the whole furnace.

B. Description of the Furnace

Figure 1 shows a sketch of the actual glass furnace, which is of the Pittsburgh kind.

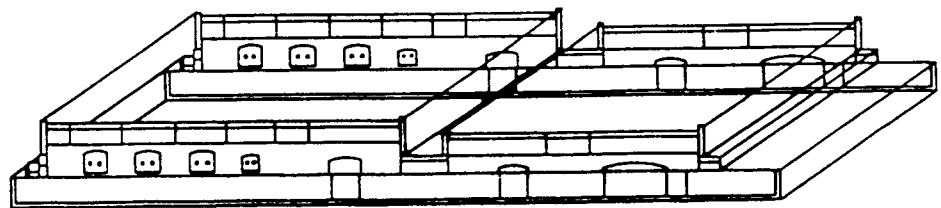


Fig. 1 Sketch of the furnace.

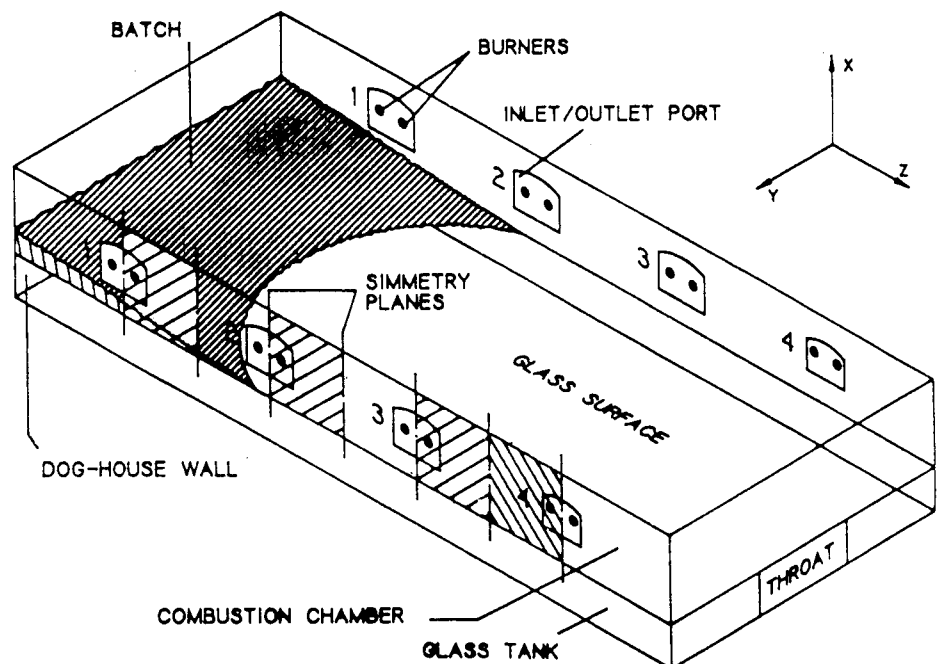


Fig. 2 Calculation domain.

Figure 2 shows a sketch of the furnace region on which the numerical geometry is based, which is essentially a large insulated container in which the batch enters via the doghouse and the molten glass flows from the doghouse near-wall to the opposite endwall. The firing ports are located along the sides of the furnace. There are four ports on each side, each port containing two fuel jets. The furnace is fired alternately from either side to give more uniform heat flux to the glass and to make regeneration possible. The combustion products pass through regenerators that are used to preheat the combustion air before it enters the furnace to produce higher temperatures and heat flux to the glass. Waste ports opposite burners working as outlet ports are demanded by the reversing operating conditions. Heavy oil is burned with excess of air. Upper and side walls of the furnace are refractory-lined.

II. The Physical Modeling

The present modeling problem in its entirety has two distinct parts: the simulation of the combustion chamber and the simulation of the glass tank. We have treated these separately, with the aid of different numerical solution procedures. The simulation of the whole furnace is a hybrid treatment involving the two codes. Details of these models can be found in Carvalho et al. (1988-b).

A. The Combustion Chamber

The governing transport equations for the mean motion of a turbulent three-dimensional reacting flow were applied in their cartesian co-ordinate form.

The Mean Flow Equations. The time-averaged equations for the conservation of momentum were used as well as the equation for the conservation of energy. In addition to the referred equations, one must also include the equation of mass continuity.

The Turbulence Model. The "two-equation" model (Launder and Spalding 1972), in which equations for the kinetic energy of turbulence k and its dissipation rate ϵ are solved, was considered appropriated.

The Combustion Model. The combustion model is based on the ideal of a single step and fast reaction between the gaseous fuel and oxidant, assumed to combine in stoichiometric proportion. Equal effective turbulent mass diffusion coefficients for the fuel and oxidant and an instantaneous reaction are also assumed [see Pun and Spalding (1967); Bilger (1980)].

The transport equation for the mixture fraction f was solved.

Furthermore, we have assumed that the chemical kinetic rate is fast with respect to the turbulent transport rate; then fuel and oxidant cannot coexist, so $m_{fu} = 0$ for $m_{ox} \geq 0$ and $m_{ox} = 0$ for $m_{fu} \geq 0$, and the concentrations m_{fu} and m_{ox} are related linearly to the mixture fraction.

The above modeling, it may be noted, presumes a stationary thin-flame envelope. The fluctuating nature of the turbulent reaction is more usually accommodated (e.g., in the work of Spalding 1971) through a modeled equation for the variance of the mixture fraction fluctuations.

We have adopted a statistical approach to describe the temporal nature of the mixture fraction fluctuations. In the present work we have assumed the "clipped normal" probability density function (Lockwood and Naguib 1975), which is characterized by just two parameters: f and the mean square of the f fluctuations $g = (f - \bar{f})^2$.

Particular attention was given to radiation because it plays a dominant role in the heat transfer process inside industrial furnaces, and a simple and economical model for oil-fired furnaces was used in which it was assumed that the oil spray evaporates instantaneously.

The Soot Model. The distinctive feature of oil-fired flames is their significant soot content. Soot is of concern because its presence greatly augments the radiation heat transfer and because it is a pollutant. To predict the spacial distribution of soot, a transport equation of its mass concentration was solved. To characterize soot production, a simple global expression similar to that used by (Khan and Greeves 1974) was chosen. A straightforward method of estimating the rate of soot burning proposed by (Magnussen and Hjertager 1976) was used in the present work.

The Radiation Model. The "discrete transfer" radiation prediction procedure of (Lockwood and Shah 1981) was utilized in this study. This method combines ease of use, economy, and flexibility of application. This last feature is of particular importance in the real world of geometrically intricate combustion chambers.

The gas absorption coefficient was calculated from the "two grey plus a clear gas" fit of Truelove (1976). Water vapor and carbon dioxide are the prime contributors to the gaseous radiation.

B. The Glass Tank

The governing transport equations of the three-dimensional laminar flow driven by free convection were applied in their cartesian co-ordinate form.

The Governing Equations. The conservation of momentum may be written, in tensor notation, as follows:

$$\frac{\partial}{\partial x_j} [\rho u_j u_i + p \delta_{ij} - \mu (\frac{\partial u_i}{\partial x_j} + \frac{\partial u_j}{\partial x_i} - \frac{2}{3} \frac{\partial u_k}{\partial x_k} \delta_{ij})] - \rho g_i \beta (T - T_o) = 0 \quad (1)$$

where β is the volumetric coefficient of thermal expansion, and T_o is a reference temperature. The last term of this equation represents the buoyancy term.

The energy equation is

$$\frac{\partial}{\partial x_j} (\rho u_j T) - \frac{\partial}{\partial x_j} (\Gamma_T \frac{\partial T}{\partial x_j}) - S_T = 0 \quad (2)$$

and the continuity equation is given by

$$\frac{\partial}{\partial x_j} (\rho u_j) = 0 \quad (3)$$

The property values, varying with temperature, were calculated by special functions, as described below.

The dynamic viscosity was calculated by the Fulcher-Vogel-Tamman equation (Stanek 1977):

$$\mu = \exp(-A + \frac{B}{T - T_o}) \quad (4)$$

where A , B , and T_o are constants calculated from (COVINA Laboratories 1986).

The density was calculated from the following equation (Stanek 1977):

$$\rho = \rho_o [1 - \beta (T - T_o)] \quad (5)$$

where ρ_o is the density of the molten glass at the temperature T_o .

The radiation transfer was handled by the Rosseland (optically thick) approximation, which results in appropriately augmented thermal conductivities in the energy balance equation. From, the work of Tooley (1974), the thermal conductivity was given by

$$K_{eff} = (C_1)_k T^3 \quad (6)$$

where $(C_1)_k$ is a constant calculated from a report from COVINA Laboratories (1986).

It was assumed from experimental observation that the batch region, which is a mixture of raw material (sand) and recycled glass, forms a thin layer covering the molten glass from the doghouse (batch inlet door) until the second burner. It was also assumed that the batch temperature varies linearly between the inlet batch temperature and the melting temperature of the batch.

III. The Numerical Solution Procedure

A. Preliminary Considerations

The combustion chamber and the glass tank were simulated separately by different numerical solution procedures used as a hybrid treatment to simulate the whole furnace.

Nearly all industrial furnaces are three-dimensional and exhibit the disparity of scales, in that most of the combustion takes place within a volume surrounding the burner, which occupies only a small proportion of total furnace volume but requires a disproportionately large portion of the total computational grid.

To avoid excessive memory requirement, the combustion chamber is assumed to consist of slices. Each slice is contained between the midway plane of one inlet port and the midway plane between this inlet port and the neighboring one. As shown in Fig. 2, there are four inlet ports with two burners in each one, which makes eight slices to simulate the whole combustion chamber.

In the work of Megahed (1978), the combustion chamber was divided into several slices, but only two were calculated: the first representing the region over the molten glass and the second simulating the region over the batch. However, in the present case the inlet conditions differ significantly from one port to another (see Table 1), and

Table 1 Inlet conditions

Port no. (Fig. 2)	1	2	3	4
Total fuel flow (Kg/h)	327	496	496	175
Total air flow (Kg/h)	5480	8100	8680	3810
Excess air (%)	14	11	19	48
Fuel velocity (m/s)	0.505	0.765	0.765	0.27
Air velocity (m/s)	4.23	6.34	6.70	2.94

the overall performance of the combustion chamber was obtained by studying four slices (each one containing different inlet ports).

Because of the large period of time between the changes of side-firing in the furnace, the cycling nature of the firing process was neglected.

The glass tank predictions were made for the entire volume because they did not demand particular refinement of the grid.

B. Method of Solution

The finite difference method used to solve the equations entails subdividing the combustion chamber and the tank into a number of finite volumes or "cells." Both solution algorithms are embodied in versions of TEACH program (Gosman et al. 1976) for three-dimensional recirculating flows. The convection terms were discretized by the hybrid central/upwind method (Spalding 1972).

In the combustion chamber predictions, the velocities and pressures are calculated by a variant of the SIMPLE algorithm described in the work of Caretto et al. (1972).

In the tank flow predictions, the velocities and pressure are calculated by a variant of the PISO algorithm presented by Issa (1982). The use of PISO results in a substantial reduction in computing effort over that required by iterative methods (Issa et al. 1983).

The solution of the individual equations sets was obtained by a form of Gauss-Seidel line-by-line iteration, in both submodels.

IV Presentation and Discussion of the Results

A. Some Computational Details

The present prediction procedure has been applied for the solution of the process in a full-scale industrial glass furnace with the real operating conditions. The daily production of the glass, or the throughput, is 100 tones.

As described in Sec. 3, the furnace contains four firing ports. The total mass flow of fuel and air at each port can be found in Table 1, which presents the normal operating conditions of the furnace (designated in the present work as "RUN 1").

The fuel is injected at 393°K and the air is pre-heated to be injected at 1273°K . The fuel composition is 86% carbon and 14% hydrogen. The inlet axial velocities of fuel

and air can be found on Table 1. The radial and tangential velocities were set to zero due to absence of swirl.

The kinetic energy of turbulence at the inlet k_{in} was assumed to be 0.3% of the kinetic energy of the mean flow, and its dissipation rate (ϵ_{in}) was calculated from the relation

$$\epsilon_{in} = \frac{6.0 k_{in}^{1.5}}{\ell}$$

where ℓ is a characteristic length scale.

Each port operates under different combustion conditions. The excess air can be found at the referred table. These conditions provide a transversal heat flux distribution with a maximum value between the second and the third burner. A given glass temperature distribution, calculated by the glass tank submodel, was used for the furnace combustion chamber predictions.

Part of the upper surface of the molten glass is covered by a batch blanket. Close to this solid surface, the tangential velocity is set to zero due to the nonslipping interface fluid-solid condition. In the remaining part of the referred surface, the velocity is calculated from a vanishing shear-stress condition. A given parabolic profile was used for inlet velocities (Oliveira 1986). For the outlet (glass flowing through the throat channel), stream-wise velocity gradients were set to zero. The heat flux, calculated by the combustion chamber submodel, was used to predict the glass tank operating conditions.

Overall heat transfer coefficients were calculated based on the building material thickness and external cooling conditions given by a report from COVINA Laboratories (1986). These values vary from 1.9 to 7.1 W.m⁻².K⁻¹.

For the combustion chamber predictions a numerical grid comprising 14 x 10 x 14 grid nodes in the x, y, and z co-ordinate directions, respectively, was used, simulating each half-port slice of the furnace, whereas for the whole glass tank predictions a 14 x 16 x 27 grid was used.

Calculations for the whole furnace were made by the following procedure:

- 1) A slice of the combustion chamber corresponding to one of the half-ports (Fig. 2) was predicted, assuming a glass surface temperature distribution. The results obtained were used as initial values to predict the remaining three half-port slices of the combustion chamber. For RUN 1, 300 iterations were needed [38 central processing unit (CPU) hours in a MicroVax II] to achieve convergence for the first half-port slice (the results were considered converged when

Table 2 The parameters investigated (the values are referred to the third slice of the combustion chamber)

RUN	Excess air (%)	Air preheating ($^{\circ}\text{K}$)	Burner axis distance from the floor (m)	Investigated parameter
1	19	1273	0.35	Standard run
2	19	1373	0.35	The effect of air preheating
3	19	1173	0.35	
4	25	1273	0.35	The effect of the excess air
5	0	1273	0.35	
6	19	1273	0.7	The position of the fuel jet

the normalized residuals of the equations were less than 5×10^{-3}). For the other slices, only 120 iterations (15 CPU hours) were needed.

2) With the fluxes to the glass, calculated from the previous runs, the whole glass tank was predicted, with the same convergence criteria, which takes 120 iterations (13 CPU hours in the same computer).

3) The temperature distribution of the glass surface was then used to repeat the whole process from step 1.

4) The procedure was considered converged when the glass surface temperatures and the fluxes to the glass did not vary by more than 10% from one cycle to the next one. At the end of the fourth cycle "convergence" was achieved.

The conditions described before (see Table 1) were used as the standard run (RUN 1), which defines the operating conditions of the furnace. This study was directed toward the improvement of the actual design and operating conditions of the furnace. Several runs were made for an optimization of the combustion chamber operating conditions. The effect of operating conditions such as excess air and preheat were studied, and the best position of the fuel jet was sought. Table 2 shows a summary of the parameters under investigation.

B. Discussion of the Results

Validation of furnace predictions against experimental data acquired in a full-scale industrial glass furnace with the real operating conditions is a very important task. In spite of that, measurements are very uncommon because it is difficult to obtain them due to severe conditions of high

temperature and corrosion levels occurring inside the furnaces.

A few outlet data values are given in a report by COVINA Laboratories (1986) and are compared with the predicted values in Table 3.

As can be seen, the predicted values do agree quite well with the very few experimental ones. In spite of the lack of good quantitative validation evidence, the trends in the results show that the performance of this furnace is well-characterized by the mathematical model. In the numerical treatment of this furnace, some sources of inaccuracy may be presented. The interaction between two neighboring flames is neglected. The application of the hybrid central/upwind scheme may lead to numerical diffusion. The sources of error together with the simplicity of the turbulence and combustion model have proved to be minor in previous application (Carvalho et al. 1988-a). Indeed, the combustion chamber models used herein are the same as those used by Carvalho et al. (1988-a), where extensive validation of the predictions against experimental data acquired in a real furnace were made. The results have shown good agreement between both. This is a consequence of the importance of the radiation in large industrial furnaces.

Table 3 Outlet port no. 3 data (RUN 1)

Variable	Experimental values	Predicted values
Outlet velocity (m/s)	8.30	8.60
Outlet temperature ($^{\circ}$ K)	1720	1710
Outlet CO ₂ mass concentration	0.14	0.15
Outlet O ₂ mass concentration	0.034	0.04

Table 4 Predicted performance criteria of the furnace

RUN	Energy input (KW)			Total heat flux to the glass (KW)	Outlet temperature ($^{\circ}$ K)
	Air	Fuel	Total		
1	1596	2826	4422	980	1710
2	1720	2826	4546	1032	1865
3	1470	2826	4296	831	1790
4	1797	2826	4623	940	1840
5	1436	2826	4262	925	1817
6	1596	2826	4422	983	1720

Table 4 illustrates some aspects of the comparative study of the combustion chamber performance for the parameters under investigation. Figures 3 to 6 show, respectively, the temperature distribution and fuel, oxygen, and carbon dioxide concentrations for each run on the vertical plane containing the burner and normal to the inlet/outlet port. Figure 7 shows the fuel concentration on the nearest plane parallel to the outlet port, which is the last plane calculated by the model. The effects on the furnace of varying the air preheat and excess air levels, relative to the actual conditions (RUN 1), are described below.

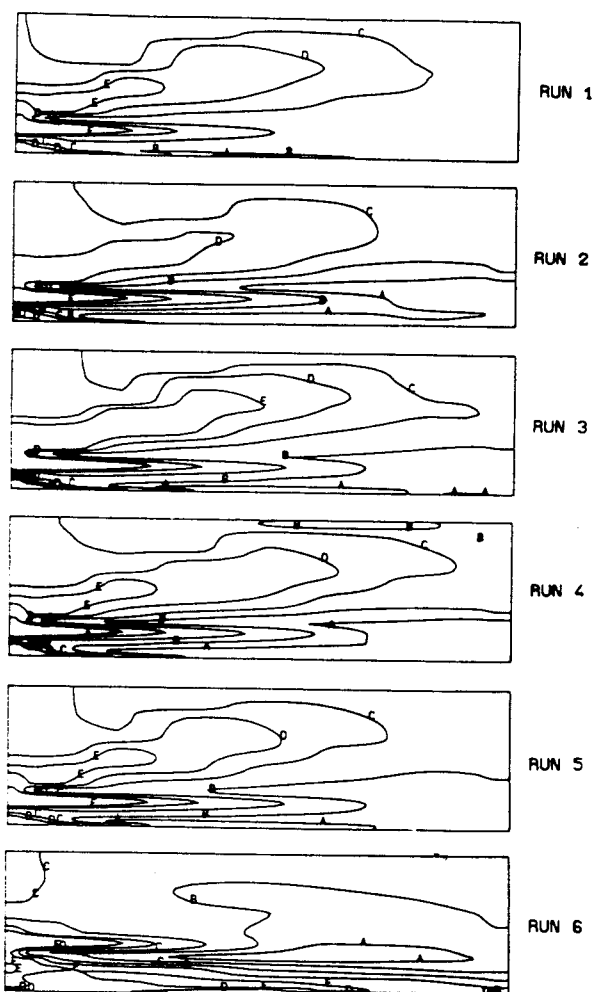


Fig. 3 Temperature distribution ($^{\circ}\text{K}$) for all studied cases (combustion chamber; $Z=0.43$ m): A=1880, B=1800, C=1650, D=1450, E=1300.

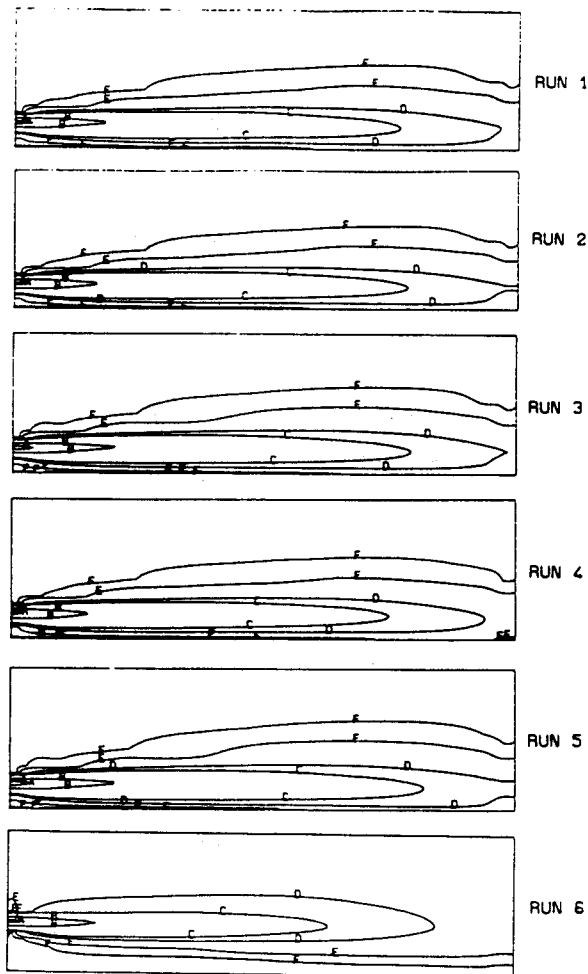


Fig. 4 Fuel mass concentration for all studied cases (combustion chamber; $Z=0.43$ m): $A=0.80$, $B=0.50$, $C=0.10$, $D=0.05$, $E=0.008$, $F=0.0005$.

1. Effect of the Air Preheating. The effect of the air preheating can be seen by comparing cases 1, 2, and 3. Increasing the air preheat to 1373°K (RUN 2) increases the gas temperature field (Fig. 3). The fuel, oxygen, and carbon dioxide concentrations do not vary significantly, as shown by Figs. 4 to 6. As a consequence of the higher levels of the gas temperature, the total heat flux to the glass increases (see Table 4) as well as the outlet temperature. The decrease of air preheat to 1173°K (RUN 3) decreases the gas temperatures inside the combustion chamber. Figure 7 shows that the level of air preheat does not influence significantly the wasted unburned fuel at the outlet.

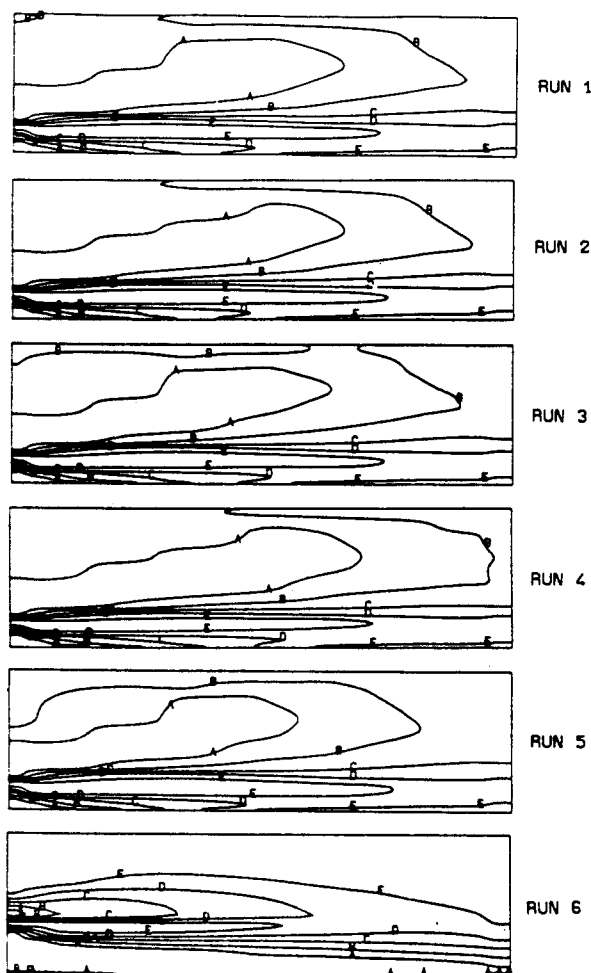


Fig. 5 Oxygen mass concentration for all studied cases (combustion chamber; $Z=0.43$ m): $A=0.20$, $B=0.15$, $C=0.10$, $D=0.06$, $E=0.02$.

2. Effect of the Excess Air. The effect of the excess air can be determined by comparison of cases 1, 4, and 5. Both the increase of the excess air to 25% (RUN 4) and the decrease to the stoichiometric proportion (RUN 5) lead to a reduction of the total heat flux to the glass (Table 4) and an increase of the outlet temperature. Figures 4 to 6 show that the fuel, oxygen, and carbon dioxide concentrations have no qualitative differences. However, the wasted unburned fuel varies indirectly proportional with excess air in both RUN 4 and RUN 5, as shown by Fig. 7. The temperature levels inside the combustion chamber are higher for RUN 4 due to a more efficient combustion (Fig. 3).

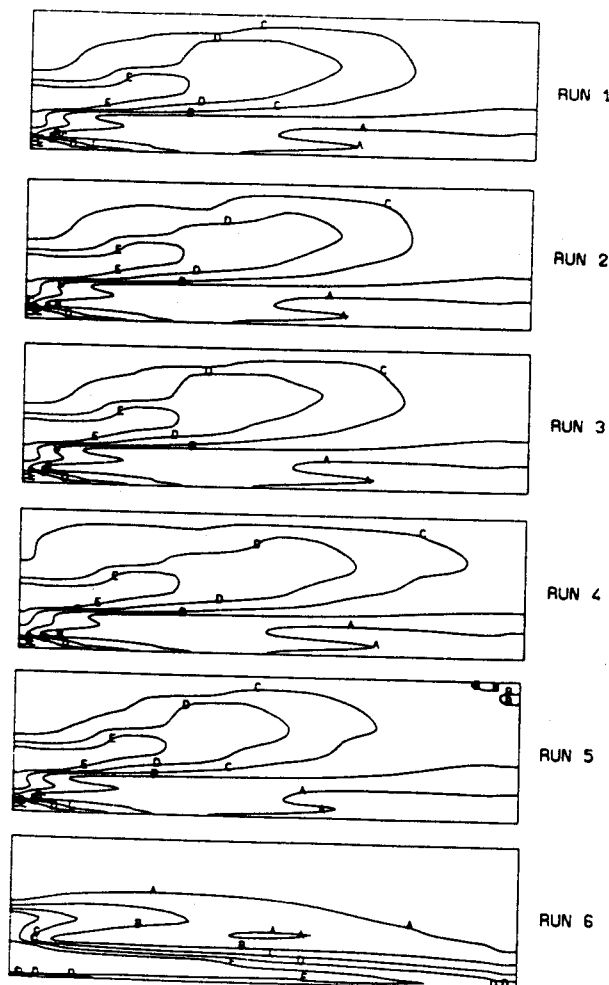


Fig. 6 Carbon dioxide mass concentration for all studied cases (combustion chamber; $Z=0.43$ m): $A=0.15$, $B=0.10$, $C=0.06$, $D=0.03$, $E=0.01$.

The results described above confirm the poor mixing pattern between oxygen and fuel in the present geometry. Figure 5 shows that, in the cases observed (RUN 1 to RUN 5), there is a considerable amount of unused oxygen in the upper region of the furnace, where there is no fuel (Fig. 4), and some unburned fuel leaves the furnace (Fig. 7). A better performance of the furnace was sought by changing the fuel injection position.

3. Effect of the Position of the Fuel Jet. The influence of the position of the fuel jet on the resulting flow and temperature fields and mass fraction distributions can be assessed by comparing RUN 1 with RUN 6. For RUN 6, the fuel injection distance to the glass surface was duplicated.

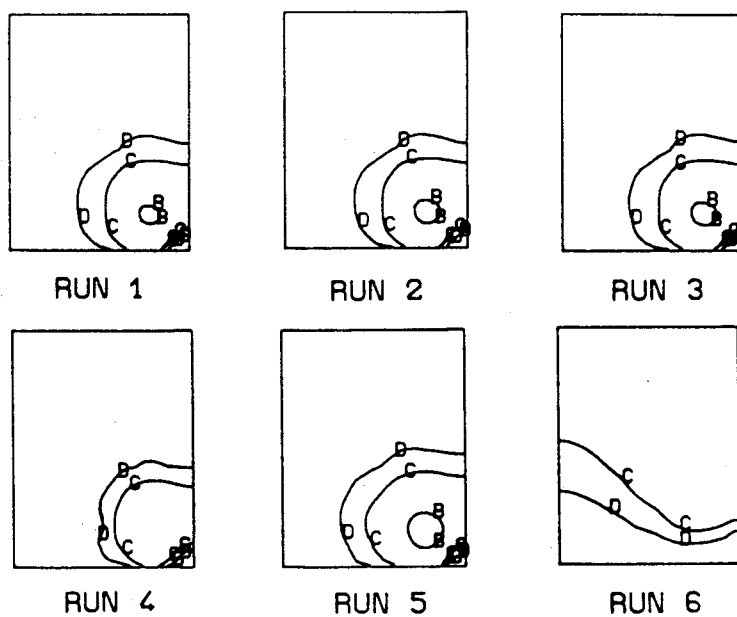


Fig. 7 Fuel mass concentration for all studied cases at the outlet port (combustion chamber; $Y=7.00$ m): $B=0.05$, $C=0.005$, $D=0.0005$.

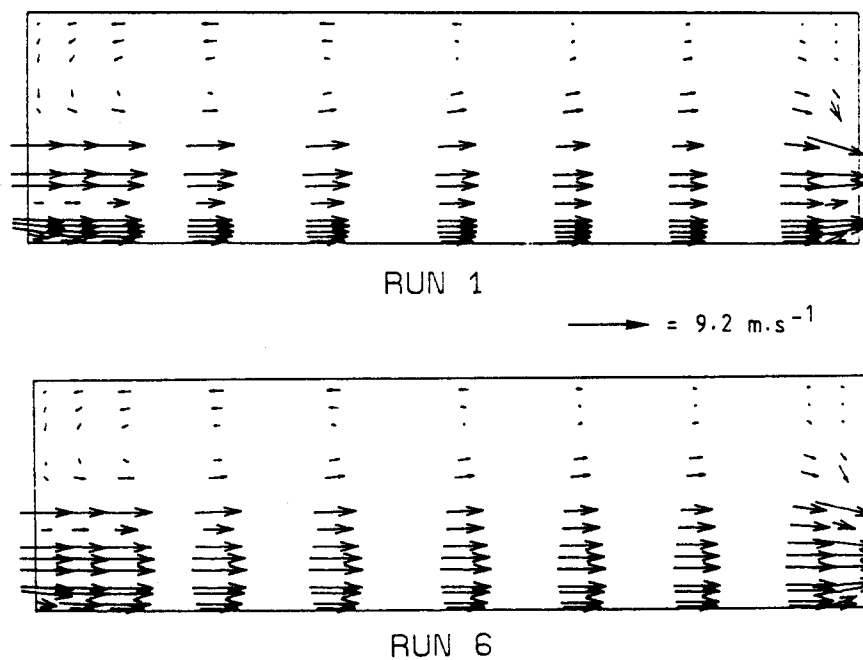


Fig. 8 Velocity vectors for RUN 1 and RUN 6 (combustion chamber; $Z=0.43$ m).

For this case, the furnace displays a much better performance.

The maximum temperatures in the combustion chamber (Fig. 3) moved up from the region near the glass surface, which proves that the fuel jet is no longer deviated toward the glass. Figure 4 confirms this fact because the fuel concentration near the glass (RUN 6) became almost zero. Another important improvement was the fact that the fuel concentration at the outlet is almost zero (Fig. 7).

The mixing pattern of the reactants was improved because there is no more unused oxygen in the upper region of the furnace (Fig. 5). The carbon dioxide concentration is maximum where the reaction takes place, which confirms the results described above.

A few more results are illustrated in Figs. 8 to 10, which show some aspects of the flow pattern and flame shape for RUN 1 and RUN 6. Figure 8 shows the velocity vectors projected on a vertical plane normal to the inlet port containing the burner. The flow pattern is similar, apart from the different location of the fuel injection.

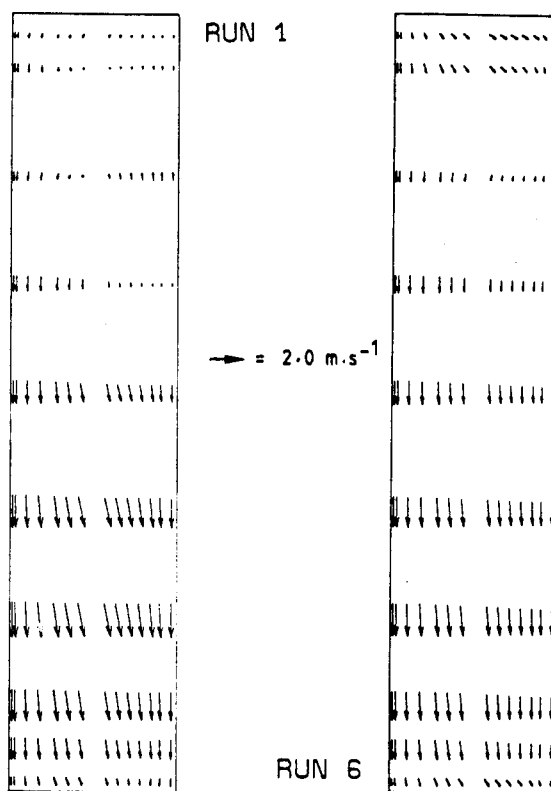


Fig. 9 Velocity vectors for RUN 1 and RUN 6 (combustion chamber; $X=1.90 \text{ m}$).

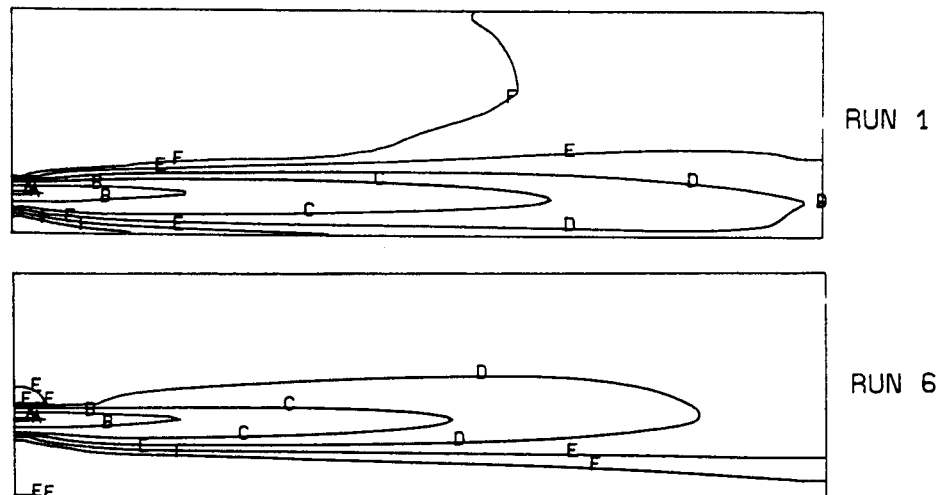


Fig. 10 Mixture fraction distribution for RUN 1 and RUN 6 (combustion chamber; $Z=0.43$ m): $A=0.80$, $B=0.50$, $C=0.20$, $D=0.10$, $E=0.05$, $F=0.025$.

Figure 9 shows the flow in the horizontal plane near the roof of the furnace. The upper recirculation zone is extended to the whole furnace in the case of RUN 6 as the flow is inverted in its total width and length. For RUN 1, Fig. 9 shows that this total inversion occurs only in the left part of the furnace, whereas in the right half the recirculation occupies only two thirds of the total length.

Figure 10 shows the mixture fraction in the same plane as Fig. 8. The flame length for RUN 6 (based on the "chemical definition," i.e., the distance from the burner of stoichiometric mixture fraction) is smaller than that for RUN 1. Values for the flame length for RUN 6 and RUN 1 of 6.2 m and 6.8 m, respectively, were predicted against a value of 6.5 m obtained from experimental observation.

V. Concluding Remarks

This paper has described the application of a very useful and general prediction procedure to the improvement of the design and operating conditions of a full-scale industrial glass furnace. From this study it appears that the present furnace design is not the best and that many improvements can be achieved with minor changes. The mixing pattern is not very efficient due to the inlet port geometry and the combustion chamber aerodynamics. The cross-stream velocities around the fuel jet are directed in such a way to carry the fuel away from air and toward the glass. The change of the fuel jet position, as made in RUN 6, prevents

this phenomena because the low pressure inside the recirculation zone pulls the fuel away from the glass, allowing a much better mixing between the fuel and the air. In this way the usability of air input is increased, and no wasted unburned fuel leaves the furnace.

Acknowledgments

The authors wish to acknowledge COVINA Laboratories for technical advice. The final manuscript was completed with the help of M. Cristovão, F. Farinha, and Rui Ferreira.

References

- Bilger, R. W. (1980) Turbulent flows with non-premixed reactants, turbulent reacting flows. Topics in Applied Physics, Springer-Verlag, Berlin, FRG. (edited by P. A. Libby and F. A. Williams).
- Caretto, L. S., Gosman, A. D., Patankar, S. V., and Spalding, D. B. (1972) Two calculation procedures for steady, three-dimensional flows with recirculation. Proceedings of the Third International Conference on Numerical Methods in Fluid Dynamics, p. 60. Springer-Verlag, New York.
- Carvalho, M. G. (1983) Computer simulation of a glass furnace, Ph.D. Thesis, University of London, UK.
- Carvalho, M. G., Durão, D. F. G., Heitor, M. V., Moreira A. L. N., and Pereira, J. C. F. (1988-a) The flow and heat transfer in an oxy-fuel glass furnace. First European Conference on Industrial Furnaces and Boilers, Lisbon, Portugal.
- Carvalho, M. G., Durão, D. F. G., and Pereira, J. C. F. (1987) The prediction of the flow, reaction and heat transfer in an oxy-fuel glass furnace. Int. J. Comput. Aided Eng. Software, 4, 23-31.
- Carvalho, M. G. and Lockwood, F. C. (1985) Mathematical simulation of an end-port regenerative glass furnace. Proc. Inst. Mech. Eng., 199, C2, 113-120.
- Carvalho, M. G., Oliveira, P., and Semião, V. (1988-b) A three-dimensional modeling of an industrial glass furnace. To be published in J. Inst. Energ.
- Chen, T. and Goodson, R. E. (1972) Computation of three-dimensional temperature and convective flow profiles for an elective glass furnace. Glass Technol., 13, 161-167.
- COVINA Laboratories (1986) Batch melting and furnace data. Report of COVINA Laboratories, Lisbon, Portugal.
- Gosman, A. D., Humphrey, J. A. C., and Vlachos, N. S. (1976) TEACH-3E: A general computer program for three-dimensional

- recirculating flows. Report CHT/76/10, Mechanical Engineering Department, Imperial College, London, UK.
- Gosman, A. D., Lockwood, F. C., Megahed, I. E. A., and Shah, N. G. (1980) "The prediction of the flow reaction and heat transfer in the combustion chamber of a glass furnace", AIAA Paper-80-0016, AIAA 18th Aerospace Sciences Meeting, CA.
- Issa, R. I. (1982) The solution of fluid flow equations operator splitting. Report No FS/82/15, Mechanical Engineering Department, Imperial College, London, UK.
- Issa, R. I., Gosman, A. D., and Watkins, A. P. (1983) The computation of compressible and incompressible recirculating flows by a non-iterative implicit scheme. Report FS/83/8, Mechanical Engineering Department, Imperial College, London, UK.
- Khan, I. M. and Greeves, G. (1974) A method for calculating the formation and combustion of soot in diesel-engines. Heat Transfer in Flames, Scripta Book Co. (edited by N. H. Afgan and S. M. Beer) pp. 391-402.
- Launder, B. E. and Spalding, D. B. (1972) Mathematical Models of Turbulence. Academic, New York.
- Lockwood, F. C. and Naguib, A. S. (1975) The prediction of the fluctuations in the properties of free, round jet, turbulent diffusion flame. Combust. Flame, 24, 109.
- Lockwood, F. C. and Shah, N. G. (1981) A new radiation solution method for incorporation in general combustion prediction procedures. Eighteenth Symposium (International) on Combustion, The Combustion Institute, Pittsburgh, PA.
- Magnussen, B. F. and Hjertager, B. H. (1976) On mathematical modeling of turbulent combustion with special emphasis on soot formation and combustion. Sixteenth Symposium (International) on Combustion, The Combustion Institute, Pittsburgh, PA.
- Mase, H. and Oda, K. (1980) Mathematical model of glass tank furnace with batch melting process. J. Non-Cryst. Solids, 38, 39, 807-812.
- McConnell, R. R. and Goodson, R. E. (1979) Modeling of glass furnace design for improved energy efficiency. Glass Technol., 20, 100-106.
- Megahed, I. E. A. (1978) The prediction of three-dimensional gas-fired combustion chamber flows. Ph.D. Thesis, University of London, UK.
- Novak, J. D. (1980) Application of combustion space energy calculations to commercial glass furnaces. J. Non-Cryst. Solids, 38, 39, 819-824.

- Oliveira, P. J. (1986) Convecção natural: um estudo numérico. Aplicação ao escoamento do vidro num forno tanque. M.Sc. Thesis, University of Lisbon, Portugal.
- Pun, W. M. and Spalding, D. B. (1967) A procedure for predicting the velocity and temperature distributions in a confined steady, turbulent, gaseous diffusion flame. Proceedings of the International Astronautical Federation Meeting, Belgrade, Yugoslavia.
- Semião, V. S. (1986) Simulação numérica de uma fornalha industrial. M.Sc. Thesis, University of Lisbon, Portugal.
- Spalding, D. B. (1971) Concentration fluctuations in a round turbulent free jet. Chem. Eng. Sci., 26, 96.
- Spalding, D. B. (1972) A novel finite difference formulation for differential expressions involving both first and second derivatives. Int. J. Numer. Methods Eng., 4, 557.
- Stanek, J. (1977) Electric Melting of Glass. Elsevier, Amsterdam, The Netherlands.
- Suzuki, J. (1976) Three-dimensional flow and temperature distributions in rectangular cavities. M.Sc. Thesis, University of Sheffield. UK.
- Tooley, F. V. (1974) The Handbook of Glass Manufacture, Vol. 1, Books for Industry.
- Truelove, J. S. (1976) A mixed grey gas model for flame radiation. AERE Harwell Report HL 76/3448/KE, Atomic Energy Authority, Oxfordshire, UK.